Microbiome

RESEARCH

Open Access

Neonates exposed to HIV but uninfected exhibit an altered gut microbiota and inflammation associated with impaired breast milk antibody function

Audrey Byrne[1], Christian Diener[2,5], Bryan P. Brown[1], Brandon S. Maust[1], Colin Feng[1], Berenice L. Alinde[3,10], Sean M. Gibbons[2,6,7,8], Meghan Koch[4,9], Clive M. Gray[3,10], Heather B. Jaspan[1,10,11] and Donald D. Nyangahu[1,11,12,13,14*]

Abstract

Background Infants exposed to HIV but uninfected have altered immune profiles which include heightened systemic inflammation. The mechanism(s) underlying this phenomenon is unknown. Here, we investigated differences in neonatal gut bacterial and viral microbiome and associations with inflammatory biomarkers in plasma. Further, we tested whether HIV exposure impacts antibody-microbiota binding in neonatal gut and whether antibodies in breast milk impact the growth of commensal bacteria.

Results Neonates exposed to HIV but uninfected (nHEU) exhibited altered gut bacteriome and virome compared to unexposed neonates (nHU). In addition, HIV exposure differentially impacted IgA-microbiota binding in neonates. The relative abundance of *Blautia* spp. in the whole stool or IgA-bound microbiota was positively associated with plasma concentrations of C-reactive protein. Finally, IgA from the breast milk of mothers living with HIV displayed a significantly lower ability to inhibit the growth of *Blautia coccoides* which was associated with inflammation in nHEU.

Conclusion nHEU exhibits profound alterations in gut bacterial microbiota with a mild impact on the enteric DNA virome. Elevated inflammation in nHEU could be due to a lower capacity of breast milk IgA from mothers living with HIV to limit growth the of gut bacteria associated with inflammation.

Keywords Inflammation, Gut microbiota, Neonates exposed to HIV but uninfected

*Correspondence:
Donald D. Nyangahu
donaldnyangahu@gmail.com
[1] Seattle Children's Research Institute, Seattle, WA, USA
[2] Institute For Systems Biology, Seattle, WA 98109, USA
[3] Stellenbosch University, Cape Town, South Africa
[4] Basic Sciences Division, Fred Hutchinson Cancer Center, Seattle, WA 98101, USA
[5] Diagnostic and Research Institute of Hygiene, Microbiology and Environmental Medicine, Medical University of Graz, Graz, Austria
[6] Department of Bioengineering, University of Washington, Seattle, WA 98195, USA
[7] Department of Genome Sciences, University of Washington, Seattle, WA 98195, USA
[8] eScience Institute, University of Washington, Seattle, WA 98195, USA
[9] Department of Immunology, University of Washington, Seattle, WA 98195, USA
[10] Division of Immunology, University of Cape Town, Cape Town, South Africa
[11] Department of Pediatrics, University of Washington, Seattle, WA 98195, USA
[12] Department of Pharmacology, The State University of New Jersey, RutgersPiscataway, NJ 08854, USA
[13] Center for Advanced Biotechnology and Medicine, The State University of New Jersey, RutgersPiscataway, NJ 08854, USA
[14] Department of Human Pathology, Egerton University, Nakuru, Kenya

Background

Due to lifelong antiretroviral treatment of pregnant mothers living with HIV, there has been a decrease in vertical transmission of HIV [1]. However, this has led to a growing population of infants who are HIV-exposed and uninfected. These infants have up to four-fold higher rates of morbidity and mortality from infections compared to unexposed infants [2, 3], possibly due to their altered immunological profiles [4] and heightened inflammation [5, 6]. The mechanism(s) behind their elevated inflammation are largely unknown. Among the factors that have been suggested to impact immune development in infants that are HIV-exposed include the developing gut microbiota. Previous studies have assessed the gut microbiota in these infants with variable results [7–9], likely due to a range of sample sizes, different modes of feeding, or cohorts from different geographical areas, all of which may impact results. These studies also utilized 16S rRNA amplification which has limited ability to discriminate species or strain level information and predict microbial function [10]. In addition to bacteria, a substantial number of viruses also colonize the human gut, collectively termed the enteric virome [11]. Beyond the bacterial microbiota, no studies have characterized the enteric virome in these infants exposed to HIV. Whether the gut microbiomes (bacteriome and virome) are associated with inflammation in infants exposed to HIV and uninfected is unknown, but a plausible explanation given the link between gut microbiome and immune development [12].

Human milk provides direct immunity through the transfer of immune components from mother to offspring [13]. Among the main factors transferred in breast milk are immunoglobulins (Igs) which are important effectors of the adaptive immune system [14]. Persons living with HIV (PLWH) have altered total immunoglobulin and subclass concentrations in serum [15, 16]. IgG abnormalities have also been reported in the serum of pregnant women living with HIV, a phenomenon that persists 24 months postpartum [17]. Few studies have examined the effect of HIV on immunoglobulin subclasses in breast milk. Previous work in murine models has shown that immunoglobulins in breast milk dampen mucosal T cell responses in the offspring through the binding of commensal gut bacteria; thus, limiting inflammatory immune responses to commensals [18]. Furthermore, IgA-coated bacteria enhance susceptibility to colitis in a mouse model [19]. In human adults, systemic IgG binds to a broad range of commensals that correlate with reduced inflammation [20]. Together, these studies suggest that microbiota-antibody interactions shape immune phenotypes. Whether HIV infection impacts immunoglobulin concentrations in breast milk and whether the passively acquired antibodies exhibit an altered microbiota coating in infants is not clear.

Here, we compare the gut bacterial microbiota and DNA virome in 4-week-old neonates exposed to HIV but uninfected (nHEU) and neonates that are HIV unexposed (nHU) using shotgun metagenomic sequencing and correlate these taxa with systemic biomarkers of inflammation. In addition, we profile IgA-coated bacteria by comparing nHEU and nHU. Finally, we assess the relationship between microbiota-specific IgA in breast milk and gut composition in neonates.

Methods

Study design and participant characteristics

Mother-infant pairs were recruited at the Midwife Obstetric Unit (MOU) in Khayelitsha, Cape Town, South Africa (InFANT study). The InFANT study has been recruiting mother-infant pairs since 2013 [21, 22]. Both mothers living with HIV (MLWH) and those living without HIV (MLWoH) and their infants are eligible. All mothers living with HIV and their infants are provided with antiretrovirals according to South Africa's guidelines [23]. All mothers provided written informed consent. In this study, which was nested within the larger InFANT study, we conducted a cross-sectional analysis of 35 MLWoH, 34 MLWH, and their infants at 4 weeks postpartum. Inclusion criteria for this substudy were MLWH with an undetectable viral load, CD4 count above 350 cells/μl, vaginal term deliveries, gestational age ≥ 38 weeks, no known tuberculosis contacts, no mastitis or cracked nipples. All babies were exclusively breastfed. Breast milk from the mothers was analyzed at week 4 postpartum. Stools and plasma from neonates were assessed at week 4 of life.

Immunoglobulin isotype and subclass concentrations in breast milk and stool

The concentration of total IgA, IgM, and IgG subclasses in breast milk and IgM, IgA, and IgG in neonatal stools were determined by ELISA. Samples were diluted in PBS containing 0.05% Tween® 20 and 0.1% bovine serum albumin (BSA). Breast milk samples were diluted 20,000-fold for IgA, 1000-fold for IgG1 and IgG2, 500-fold for IgG3 and IgG4, and 1000-fold for IgM. Fecal samples were resuspended in PBS (10 mg/ml). Homogenized stool samples were spun at 16,000 × *g* for 10 min. Supernatants were diluted 500-fold for IgA and 50-fold for IgM and IgG prior to ELISA. Absolute antibody concentrations in breast milk and stool were then determined using the human ELISA kit according to the manufacturer's instructions (STEMCELL Technologies). To determine absolute concentrations, standards were included in the assay, and ODs were fitted onto the standard curve. Plates

were read on a SpectraMax i3x Microplate Reader System at 450 nm with a correction wavelength of 650 nm.

Flow cytometry of bacteria in stool and separation of immunoglobulin-bound and unbound bacterial fractions

To determine the proportion of bacteria coated by immunoglobulins in neonatal stool, flow cytometry was performed as previously described [24]. Briefly, stool samples were resuspended in PBS by homogenization at 25 mg/mL. Samples were spun at 400×*g* to pellet large debris. Supernatants were filtered and spun at 8000×*g* for 5 min to pellet bacteria. The bacteria pellet was then resuspended in 300 µl of PBS 5% goat serum with SYTO BC (final conc 3 µM) on ice for 30 min. Samples were then stained with fluorochrome-conjugated anti-human IgA, G, and M (1:100 dilution) for 30 min on ice. After washing twice with PBS, samples were resuspended in 300 µl of acquisition buffer with DAPI (final conc 1 µg/mL) for flow cytometry analyses. The acquisition was done on a log scale with low FSC and SSC to allow the detection of bacteria.

Magnetic Associated Cell Sorting (MACS) was used to separate IgA-bound and unbound fractions. Briefly, a fraction of the SYTO BC stained sample was pelleted and stained with anti-human IgA conjugated to APC. Cells were then washed and resuspended in 300 µl of PBS containing anti-APC magnetic beads (1:6 dilution) for 30 min. Cells were washed, resuspended in PBS, and loaded onto magnetized columns. The IgA bound fraction was separated by positive selection while the flow through contained the IgA unbound fraction. Bound and unbound fractions were centrifuged and resuspended in 200 µl of PBS and used for DNA extraction.

Metagenomic library preparation and sequencing

DNA was extracted from stools or IgA-bound and unbound fractions using the PowerSoil DNA extraction kit (Mo Bio Laboratories). Concentrations were determined by Quant-IT dsDNA HS assay kit (Invitrogen, UK). DNA library preparation and sequencing were conducted at GENEWIZ, Inc. (South Plainfield, NJ, USA). NEB NextUltra DNA Library Preparation kit was used following the manufacturer's recommendations (Illumina, San Diego, CA, USA). Briefly, genomic DNA was fragmented by acoustic shearing with a Covaris S220 instrument. The DNA was end-repaired and adenylated. Adapters were ligated after adenylation of the 3′ends. Adapter-ligated DNA was indexed and enriched by limited-cycle PCR. The DNA libraries were validated using TapeStation (Agilent Technologies, Palo Alto, CA, USA), and quantified by real-time PCR (Applied Biosystems, Carlsbad, CA, USA). The sequencing libraries were multiplexed and clustered onto an S4 flowcell on an Illumina NovaSeq instrument according to the manufacturer's instructions. The samples were sequenced using a 2×150 bp Paired-End (PE) configuration.

Analysis of bacterial microbiota

Raw fastq files were trimmed and quality filtered using fastp [25]. Taxonomic assignment of the filtered reads was performed by Kraken2 and Bracken [26, 27]. Count matrix with species annotation was used for downstream analysis. Phyloseq [28] and vegan packages in R were used to calculate beta and alpha diversities between groups. We used both DESeq2 and corncob to determine differentially abundant taxa (those that overlapped the two methods) [29, 30]. HUMAnN3 was used to predict microbial function including MetaPhIAn (mpa_vJan21_CHOCOPhlAnSGB_202103), the nucleotide database ChocoPhIAn and protein database UniRef90 (v201901) [31].

Analysis of enteric DNA virome

To analyze the DNA virome, raw fastq files were quality filtered and reads mapping to the human genome (hg19 release) were removed by the KneadData (https://github.com/biobakery/kneaddata). Reads with a quality score < 20 and length < 90 bp were discarded. The remaining high-quality reads were used for metagenome assembly using the metaSPAdes assembler [32]. The concatenated assembly contained 9,161,546 contigs. Contigs were filtered by bbduk to include only those longer than 1500 bp. A total of 596,700 contigs met this cutoff. These were clustered at 95% nucleotide identity by coverM (coverm cluster) and viral contigs identified by geNomad [33]. A total of 3,643 contigs had positive viral hits. For additional viral annotation, the viral contigs were queried against the ICTV-NR database (built using the Virus Metadata Resource released September 13, 2023) by MMseqs2 [34]. The database was built as described here https://github.com/apcamargo/ictv-mmseqs2-protein-database. Quality filtered reads were then mapped to the annotated contigs by coverM (coverm genome) to obtain viral taxa abundance across samples. The resulting sample matrix was then imported into R for further downstream analysis. Analysis of alpha and beta diversities and determination of differentially abundant viral taxa was performed for the bacterial microbiota described above. VIBRANT was used for the prediction of lytic and lysogenic phage lifestyles [35].

Quantification of plasma proteins by SomaScan

Proteins were quantified in neonatal plasma using the aptamer-based SomaScan assay (SomaLogic). The aptamer-based technology for quantification of proteins

alongside its performance and characteristics has been previously described [36]. Briefly, the SomaScan platform is based on protein capture reagents called SOMAmer (Slow Off-rate Modified Aptamers) reagents. Aptamers are short single-stranded DNA sequences with hydrophobic modifications that allow for highly specific binding to target proteins. This assay was used to quantify 950 proteins in plasma according to the manufacturer's specifications. Results were normalized according to the manufacturer's recommendation and analyzed by limma in R [37].

Quantification of stool calprotectin

Human Calprotectin was quantified in stool using the L1/S100-A8/9 (ThermoFisher Scientific) ELISA kit according to the manufacturer's instructions.

Quantification of plasma iFABP

Human intestinal fatty acid binding protein (iFABP) was quantified in infant plasma using the FABP2 ELISA kit (ThermoFisher SCIENTIFIC) according to the manufacturer's instructions.

Purification of IgA from breast milk, bacteria growth inhibition assays, and ELISAs

IgA was purified from the breast milk of MLWH and MLWoH using the LigaTrap resin according to the manufacturer's instructions (LigaTrap TECHNOLOGIES). Purified IgA was used for bacteria growth inhibition assays.

Bacteroides thetaiotaomicron (ATCC 29148) or *Blautia coccoides* (ATCC 29236) was cultured anaerobically until log phase in chopped meat carbohydrate medium at 37 °C for 17 h. A cell suspension for each bacterial culture was then prepared (1% v/v) in a growth medium. Bacteria suspension was placed in a 96-well tissue culture plate (180 µl/ well). Twenty microliters of media alone or purified IgA from MLWoH or MLWH (final conc 6 µg/ml) was added to the bacteria suspension and plates were incubated at 37 °C in an anaerobic chamber on a cerillo plate reader. In total, we tested IgA purified from the breast milk of 10 mothers ($n=5$ MLWoH and $n=5$ MLWH). Purified breast milk IgA from each mother was tested individually in technical triplicates. Bacteria culture in the presence of media alone with no IgA was used as a positive control (6 wells total for each bacterium culture) while media alone (blank, no bacteria culture) was used as a negative control (6 wells total for each bacterium culture). Bacterial growth (ODs) was monitored at various time intervals for 24 h. A similar sample size was previously used in similar experiments testing the inhibitory capacity of IgA in inflammatory bowel disease patients [38].

To determine relative concentrations of bacteria-specific IgA in breast milk, *B. thetaiotaomicron* or *B. coccoides* cultures were heat-inactivated at 70 °C for 40 min. Nunc Maxisorp ELISA plates were coated with 10^7 CFU per 100 µl of heat-inactivated bacteria in PBS and incubated overnight at 4 °C. Plates were washed and blocked with 2% bovine serum albumin. Breast milk was diluted twofold starting at 1/3 to 1/96. Diluted breast milk samples (50 µl/ well) were added in duplicate (per dilution) and incubated at RT for 2 h. Alkaline phosphatase-conjugated anti-human IgA (STEMCELL Technologies) was added (1:1000) for an hour at RT. Plates were washed, and developed using p-nitrophenylphosphatase substrate, and optical densities were read at 405 nm.

Statistical analysis

Statistical testing of immunoglobulins, iFABP, or calprotectin concentrations was performed using Prism (GraphPad software). The Mann–Whitney U test for nonparametric data was used to compare concentrations between groups. For IgA growth inhibition assays, the average blank ODs were first subtracted from ODs of all wells containing bacterial cultures (for each bacteria culture). Compiled data for the 3 groups per bacteria was plotted using Prism. The area under the curve statistical testing was performed in prism and covered the entire duration of the bacteria culture. Repeated measures ANOVA with Tukey's correction was used to test for the statistical significance of bacteria-specific breast milk antibodies between the groups. The Welch's *t*-test was used to test the statistical significance of alpha diversity between groups while the PERMANOVA test was used for beta diversity as implemented by the R adonis2 function. In DESeq2 [30] and corncob [29] analyses, alpha was set at 0.05 and p values were adjusted for multiple comparisons by the Benjamini and Hochberg method. Taxa with adjusted p values < 0.05 from both methods were considered significantly differentially abundant.

Results

Comparable antibody distribution in breast milk between MLWH and MLWoH

We measured the concentration of total immunoglobulins and IgG subclasses in the breast milk of MLWH and those living without HIV (MLWoH) at week 4 postpartum. There was a difference in median maternal age but not number of pregnancies (Table S1A). In addition, there were no differences in median gestational age, or median birth weights for infants between mothers living with and without HIV (Table S1B). As expected, IgA was the most abundant immunoglobulin in breast milk. However, there was no difference in the concentration of breast milk IgA between MLWH and MLWoH (median

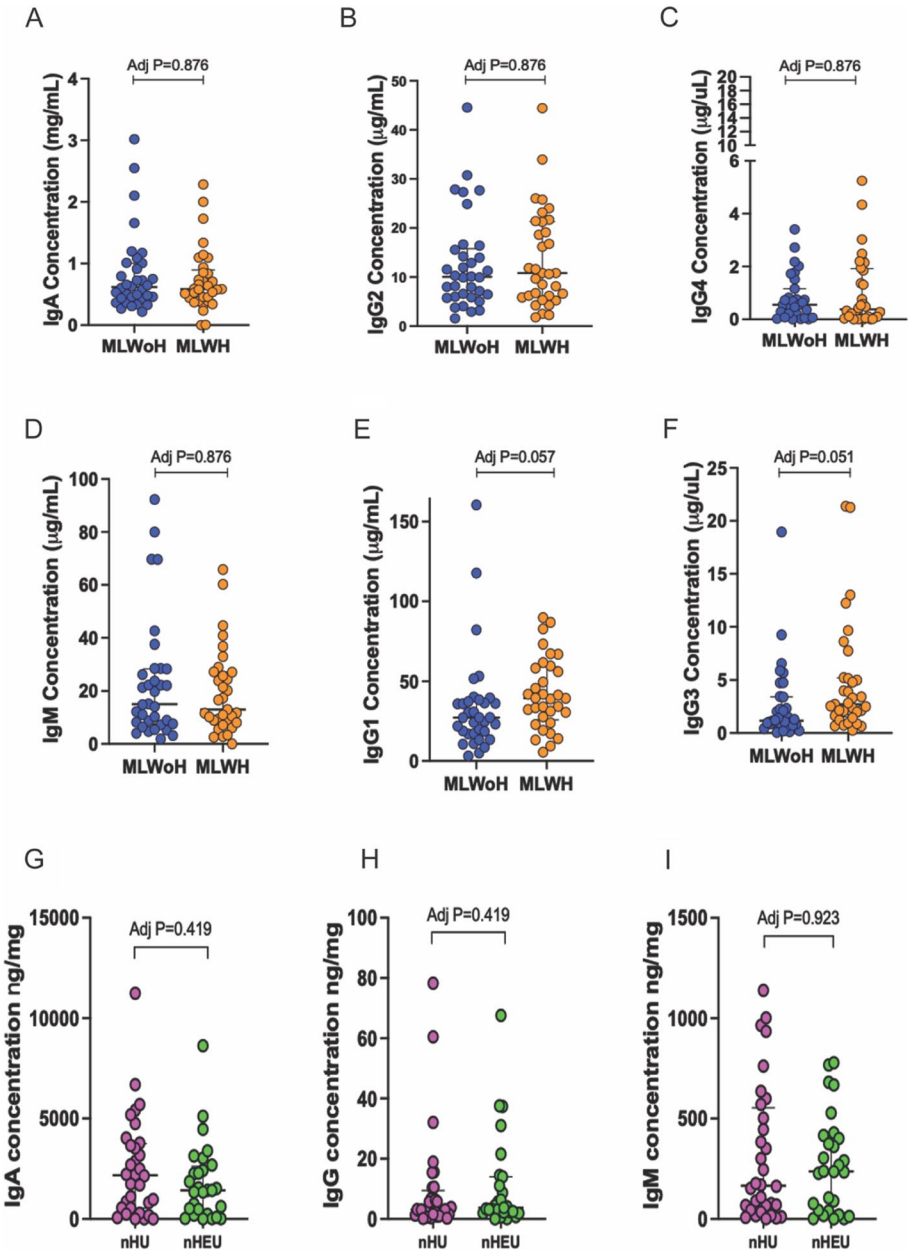

Fig. 1 Mothers living with HIV have comparable antibody concentrations to mothers living without HIV in breast milk. Total immunoglobulins were measured 4 weeks after delivery. **A**–**F** Total immunoglobulins in breast milk. **G**–**I** Total immunoglobulins in neonate's stools. Data is shown as median with interquartile range. Comparisons with *p* values < 0.05 are significant

concentration 0.61 mg/mL versus 0.58 mg/mL, Fig. 1A). Similarly, we observed no difference in the median concentrations of IgG2 (10.03 µg/mL versus 10.82 µg/mL), IgG4 (0.55 µg/mL versus 0.38 µg/mL), and IgM (15 µg/mL versus 13 µg/mL) in breast milk between MLWH and MLWoH (Fig. 1B–D). Prior to correction for multiple comparisons, total concentrations of IgG1 and IgG3 were significantly elevated in the breast milk of MLWH when compared to MLWoH (median concentration 39.30 µg/mL versus 27.25 µg/mL for IgG1, 2.703 µg/mL versus 1.167 µg/mL for IgG3, Fig. 1E–F). However, these differences did not reach statistical significance after adjustment for multiple testing (Adj $p = 0.057$ IgG1 and 0.051 for IgG3). To determine if these concentrations in breast milk influenced antibody levels in the neonate's gut, we measured total immunoglobulin concentrations in neonatal stool, at week 4 of life. As in breast milk, IgA was the most abundant immunoglobulin in stool while IgG

was the least abundant (Fig. 1G–I). However, there were no differences in the concentrations of total IgA, IgG, and IgM comparing neonates exposed to HIV (nHEU) and neonates HIV unexposed (nHU) (Fig. 1G–I). Altogether, we find that MLWH exhibits comparable antibody concentrations in breast milk to MLWoH at week 4 postpartum.

Neonates exposed to HIV (nHEU) exhibit an altered gut bacteriome compared to neonates who are HIV-unexposed (nHU)

To our knowledge, all studies thus far have used amplicon sequencing to compare the gut microbiota of all infants HEU versus HU with variable results [7–9, 39]. We used shotgun metagenomic sequencing to assess the gut microbiota of nHU and nHEU at week 4 of life, prior to the initiation of cotrimoxazole prophylaxis in nHEU [40]. An average of 64 million reads per sample were generated. After filtering low prevalence taxa (keeping taxa with at least 100 reads across 10% of samples), 2426 taxa remained that were used for downstream analysis. There was no difference in microbial alpha diversity between nHU and nHEU ($p=0.258$, Fig. 2A) using the chao1 metric. Similarly, there was no difference in Euclidean distances (PERMANOVA $p=0.327$, Fig. 2B) with approximately 30% of the variability explained on axis 1 of a Principal Component Analysis (Fig. 2B). To determine bacteria enriched in nHEU, we performed differential abundant analysis using both DESeq2 [30] and corncob [29]. We identified 43 bacterial taxa by both methods as significantly differentially abundant between nHU and nHEU (Fig. 2C, fold changes shown from DESeq2 analyses). Pathobionts including *Shigella flexneri, Shigella boydii*, and *Klebsiella pneumoniae* had a log2FC > 2 and were enriched in the stools of nHEU compared to nHU. Other notable taxa that met this criterion and were enriched in nHEU included *Blautia liquoris*, *Coprococcus eutactus,* and *Roseburia hominis*, among others (Fig. 2C). *Bifidobacterium breve* was significantly enriched in nHU compared to nHEU, as were *Actinomyces fecalis*, *Eggertella lenta,* and *Phascolarctobacterium spp.* (Fig. 2C). The gene function abundance matrix was generated using HUMAnN3 [31] and analyzed using Random Forest [41], and MaAsLin2 [42]. Random forest analysis predicted glycogen degradation, L-arginine degradation, L-methionine, and L-rhamnose biosynthesis as the most discriminative pathways and were all elevated in nHEU (Fig. 2D). Other influential pathways that predicted HIV exposure status included inosine-5-phosphate biosynthesis, lactose, and galactose degradation, and mixed acid fermentation (Fig. 2D). In the unadjusted analysis using MaAsLin2, we observed similar results to those by Random Forest. L-rhamnose biosynthesis and glycogen degradation were the top pathways elevated in nHEU. The pentose phosphate pathway, phospholipid biosynthesis, and nitrate reduction pathway were elevated in nHU (Table S2). Together, our data do not show an impact of in utero HIV exposure on microbial diversity at 4 weeks of age. However, HIV exposure alters gut bacterial microbiota composition with nHEU displaying a higher abundance of pathobionts compared to nHU. Moreover, HIV exposure impacts the functional metagenome in neonates.

HIV exposure minimally influences the enteric DNA virome

We assessed the neonatal enteric DNA virome at week 4 of life. A total of 596,700 contigs had a length equal to or greater than 1500 bp. These contigs were clustered with coverm at 95% sequence identity, yielding 196,563 OTUs. Viral contigs were then identified by geNomad [33]. The identified viral contigs were subsequently aligned by mmseqs2 against ICTV-NR database. A total of 3643 contigs were annotated as viral by geNomad. Examining the abundance of these viral taxa, there was no difference in viral alpha diversity measured by chao1 between nHEU and nHU ($p=0.140$, Fig. 3A). There was no clustering by HIV exposure status in a PCoA (PERMANOVA $P=0.171$, Fig. 3B). At the family level, Caudoviricetes were the dominant class of viruses (Fig. 3C) in both infant groups consistent with previous studies assessing early gut viromes [43]. To test for significantly enriched viral taxa, we used DESeq2 for differential abundance testing. Viruses from the genera *Peeveelvirus* (adj $p<0.0001$) were significantly enriched in nHU while *Peduovirus* (adj $p=0.001$), *Biseptimavirus (*adj $p=0.04$*)* and *Alegriavirus* (adj $p=0.003$) were significantly elevated in nHEU (Fig. 3D). These enriched viruses are phages that may be involved in the regulation of early-life bacterial microbiota. To assess whether the differentially abundant phages impact gut bacteria composition, we predicted their hosts using iPHoP [44]. The predicted hosts for *Peeveelvirus* were *Staphylococcus aureus* and *Staphylococcus agnetis*. Similar hosts were predicted for *Biseptimavirus* (Table S3). Predicted hosts for *Peduovirus* were *Escherichia coli, Escherichia fergusonii,* and *Escherichia albertii,* like those for *Alegriavirus* (Table S3). *E. coli, E. albertii*, *E. fergusonii*, and *S. aureus* were all significantly elevated in nHEU compared to nHU ($p=0.0078$, 0.0117, 0.0116, and 0.0491 respectively, Fig. 3E–H). Reports have shown that phages are abundant early in life and induced by integrated prophages [45]. Analysis of phage lifestyles predicted using VIBRANT showed a trend towards a lower number of lytic and lysogenic phages in nHEU compared to nHU, although the difference was not

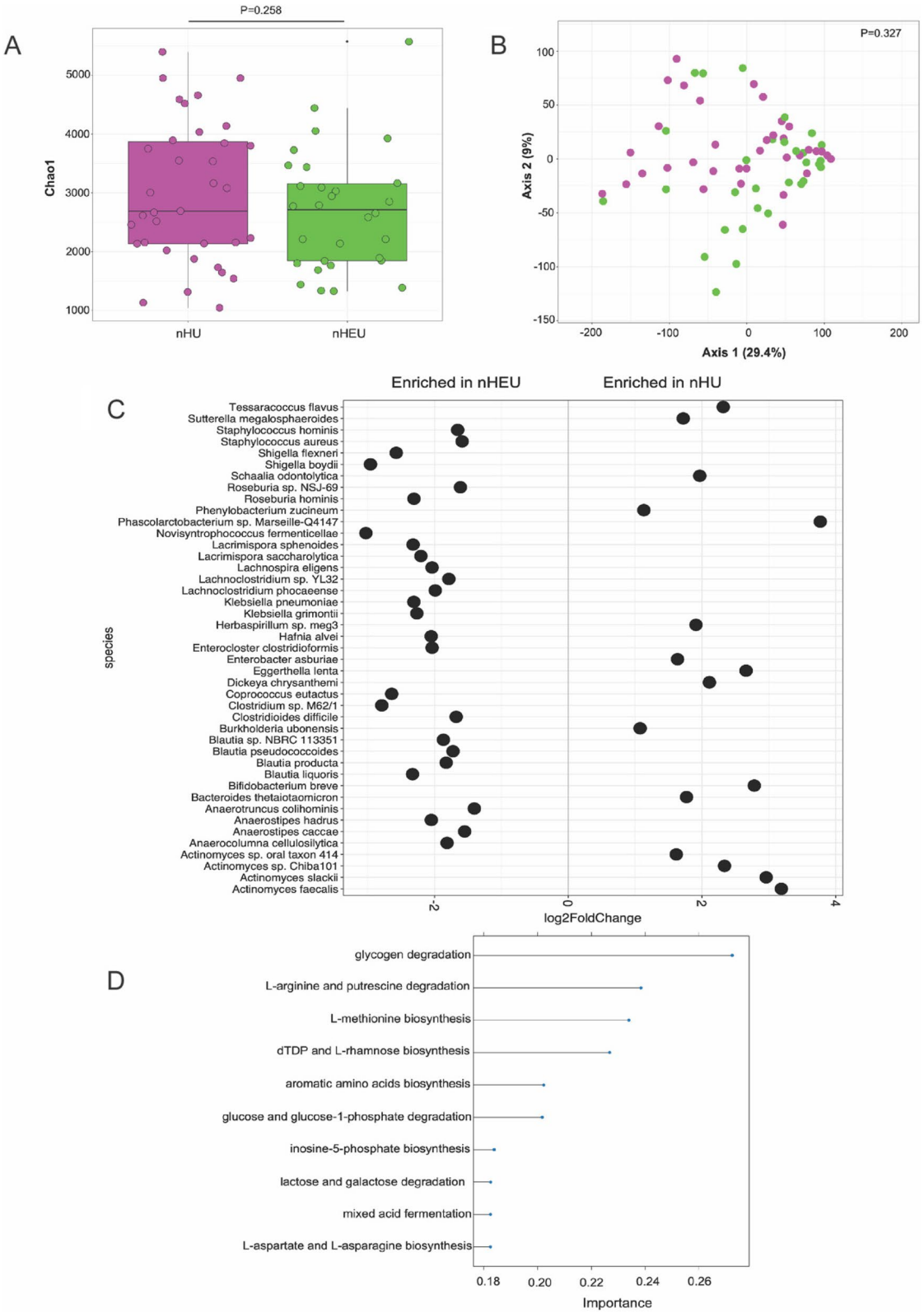

Fig. 2 HIV exposure impacts gut bacteriomein neonates. **A** Alpha diversity between neonates exposed or unexposed to HIV. **B** PCoA and PERMANOVA test of neonatal stool microbiota. **C** Differentially abundant taxa between nHEU and nHU determined by both DESeq2 and corncob. **D** Functional profiling of the microbiota by HUMAnN3

statistically significant (Fig. 3I–J). Overall, we found a modest impact of HIV exposure on the enteric DNA virome with phages elevated in nHEU predicted to infect *Escherichia spp.* Moreover, in utero HIV exposure had no significant impact on viral alpha diversity or a number of lytic or temperate phages.

HIV exposure impacts IgA microbiota coating in neonatal gut

Immunoglobulin-microbiota interactions have been shown to regulate gut homeostasis [46]. We reasoned that nHEU exhibits heightened inflammation in part due to altered immunoglobulin-microbiota interactions in the gut. Therefore, we assessed immunoglobulin-bound bacteria in the stool by flow cytometry as previously described [24]. We observed little to no IgG or IgM-bound bacteria across all infants (Fig. 4A). In contrast, a median of approximately 18% (8.6–40.2) of bacteria in nHU and 9% (3.9–44.2) in nHEU were coated by IgA, although this difference was not statistically significant ($p=0.2715$, Fig. 4A, B). We characterize the IgA + and IgA − fractions by shotgun metagenomic sequencing. The IgA + and IgA − fractions clustered distinctly by PCA but there was no clustering by HIV exposure group for either of the two fractions (Fig. 4C), suggesting differences in microbiota composition between IgA targeted and untargeted commensals. IgA bound fraction was dominated by bacteria from phylum Proteobacteria (Fig. 4D). Microbial diversity of the IgA + fraction was modestly increased in nHEU ($p=0.0508$, Fig. 4E). Using both DESeq2 and corncob (overlapping taxa by the two methods), we identified 44 taxa to be significantly differentially abundant between nHU and nHEU in the IgA + fraction (Fig. 4E). *Actinomyces faecalis,* which was also enriched in nHU whole stool (Fig. 2), was the only taxa significantly enriched in the IgA + fraction in nHU. Multiple taxa including *Bacteroides thetaiotaomicron, Blautia pseudococcoides, Bacteroides ovatus,* and *Bacteroides fragilis* were elevated in the IgA + fraction in nHEU (Fig. 4F). Bacteria generally thought of as beneficial were targeted more by IgA binding in nHEU compared to nHU. Together, we find that HIV exposure impacts IgA-microbiota coating in the gut of nHEU with a higher number of bacteria coated by IgA compared to nHU.

nHEU have heightened inflammation that correlates with gut bacterial microbiota

Gut microbiota alterations have been associated with inflammation and microbial translocation [47, 48]. Therefore, we next tested whether alterations in the gut composition of nHEU were associated with inflammatory markers in the plasma and stool. In plasma, several proteins associated with inflammation were elevated in nHEU. Specifically, C-reactive protein (CRP), an acute phase reactant [49] was significantly elevated in the plasma of nHEU compared to nHU (adj $p=0.021$, Fig. 5A). Moreover, complement factor H-related 5, a protein that regulates alternative complement activation, was significantly increased in nHEU (adj $p<0.001$, Fig. 5B). Elevated plasma concentrations of this protein have been associated with venous thromboembolism [50], and deposition in the kidneys has been associated with renal impairment [51]. Several other proteins were elevated in nHEU including Hydroxysteroid 11 Beta Dehydrogenase 1 (DHI1), an important regulator of glucocorticoids metabolism [52] (adj $p=0.022$, Fig. 5C). Furthermore, UDP glucuronosyltransferase family member A1 (UGT1.A1), an enzyme involved in conversion of bilirubin and drugs into water-soluble excretable forms [53] was elevated in nHEU suggesting elevated excretory activity possibly because these neonates are receiving antiretroviral prophylaxis (adj $p=0.031$, Fig. 5D). However, we found no difference in plasma concentration of intestinal fatty acid binding protein (iFABP), a marker of gut epithelial integrity and barrier function [54–56], between nHEU and nHU (Fig. 5E). Similarly, in stool, we observed no difference in the concentration of calprotectin, which is produced in the context of intestinal inflammation ($p=0.8833$, Fig. 5F). To test associations between systemic inflammation and the gut microbiota, we correlated the centered-log ratio (CLR) transformed relative abundance of differentially abundant bacteria in stool from Fig. 2C with proteins significantly elevated in plasma of nHEU (Fig. S1). Across all analytes, the highest correlation coefficient reported was 0.3 which was observed between specific bacterial taxa and the plasma proteins (Fig. S1). We focused our subsequent analysis on CRP which has previously been shown to be elevated in infants exposed to HIV [57]. Analysis of whole stool microbiota revealed *B. pseudococcoides* to be weakly

(See figure on next page.)

Fig. 3 HIV exposure has a modestimpact on the enteric DNA virome in neonates at week 4 of life. **A** Viral alpha diversity in stool. **B** PCoA of enteric virome constructed by Bray–Curtis distance. **C** Relative abundance of enteric virome at the family level. **D** Differentially abundant gut viruses between nHEU and nHU by DESeq2 and corncob. **E**–**H** Predicted hosts of differentially abundant phages in the guts of nHEU and nHU. **I** Total number of lytic phages between nHEU and nHU by VIBRANT. **J** Total number of lysogenic phages between nHEU and nHU by VIBRANT analysis. Comparisons with *p* values < 0.05 are significant

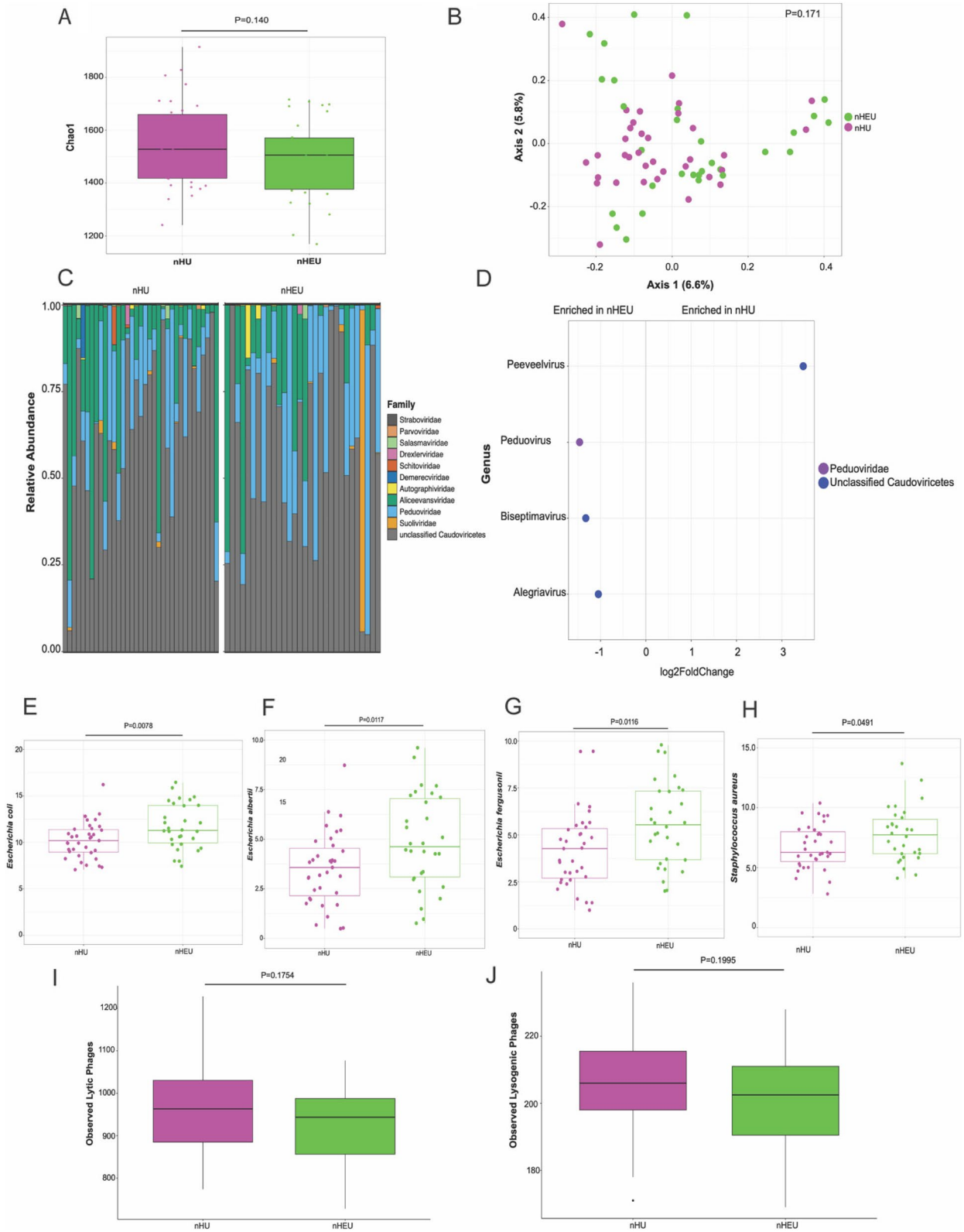

Fig. 3 (See legend on previous page.)

positively associated with CRP concentration (Fig. 6A, r = 0.32, $p = 0.047$). In addition, to test the implications of IgA-microbiota binding, we correlated CLR CLR-transformed abundance of differentially bound bacterial taxa in Fig. 4F with CRP. Two *Blautia* species (*B. producta* and NBRC 113351) bound by IgA were also weakly positively correlated with CRP concentration (Fig. 6B, r = 0.30). Our data shows that nHEU displays elevated systemic inflammation and that inflammation is weakly positively associated with the abundance of *Blautia* species.

Altered function of breast milk IgA in MLWH

IgA has been described to exhibit polyreactive specificities in the microbiota [58]. Breast milk IgA is thought to shape the assembly of the postnatal microbiota via several mechanisms including limiting the growth of specific bacteria [59]. We questioned whether IgA-microbiota interactions could have functional implications that may inform gut composition and therefore inflammation in infants. Since IgA that neonates receive at week 4 is from their mother [60], we tested the ability of breast milk IgA to inhibit microbial growth using *B. thetaiotaomicron* and *B. pseudococcoides*; both of which were enriched in the IgA + fraction from nHEU guts. We cocultured these bacteria anaerobically with IgA purified from the breast milk of MLWH or MLWoH and monitored bacterial growth. We used *B. coccoides* which is closely related to *B. pseudococcoides* for our in vitro culture experiments [61]. *B. pseudococcoides* was until recently classified as *B. coccoides* [61]. IgA from MLWoH showed superior inhibition of *B. thetaiotaomicron* growth compared to IgA from MLWH, which in turn showed more inhibition than the no IgA control (Fig. 7A). Growth inhibition of *B. coccoides* by IgA from MLWH was impaired in the exponential phase of bacteria growth compared to IgA from MLWoH (Fig. 7B). Area under the curve (AUC) analysis for the duration of bacteria culture showed significantly lower AUC when both bacteria were cultured in presence of IgA from MLWoH compared to that from MLWH ($p = 0.0051$ for *B. thetaiotaomicron* and 0.0057 for *B. coccoides,* Fig. 7C, D), suggesting a reduced ability of IgA from MLWH to inhibit commensal bacteria growth. When we analyzed levels of bacterial-specific IgA, we found no significant difference in titers of *B. thetaiotaomicron*-specific or *B. coccoides*-specific IgA between the breast milk of MLWH and MLWoH (Fig. 7E, F; adj p for *B. thetaiotaomicron* = 0.3713, adj p for *B. coccoides* = 0.4048). Altogether, these data suggest that IgA in the breast milk of MLWH exhibits significantly lower ability to inhibit growth of specific gut commensals including *Blautia* species, and therefore may lead to inflammation.

Discussion

HIV-exposed uninfected infants exhibit higher infectious morbidity, elevated immune activation, and heightened inflammation, which suggest an altered immune profile, the mechanisms of which are not clear. Here, we hypothesized that nHEU exhibits altered antibody-microbiota interactions, leading to altered gut microbiota which is associated with inflammation. We noted differences in the gut microbiota of nHEU compared to nHU by shotgun sequencing with 43 taxa being significantly differentially abundant. We observed 43 taxa to be differentially enriched in the IgA-coated stool fraction from nHEU compared to nHU. We also assessed the effect of HIV exposure on the enteric DNA virome in nHEU. Akin to the gut bacteriome, we observed no significant effect of HIV exposure on the enteric virome alpha and beta diversity although some viral taxa differed in abundance. In plasma, we noted an elevation of markers of inflammation, including CRP, in nHEU as previously described [57]. Lastly, we observed a significantly lower bacteriostatic effect of breast milk IgA from MLWH to *B. coccoides* in vitro.

Previous work reported higher total IgG1 and IgG3 in serum and other body fluids of PLWH compared to controls [62]. However, this study did not assess antibody distribution in breast milk. In our study, while these immunoglobulins were significantly elevated in the breast milk of MLWH, these differences did not reach statistical significance after correction for multiple comparisons. It is also unclear from Raux et al. whether the PLWH had suppressed viral load which could contribute to differences in our findings. Similarly, we noted no impact of HIV on total IgA and IgM, however, Lugada et al. reported significantly higher concentrations of IgA and IgM in the sera of PLWH in Uganda and Norway [16]. Although all three immunoglobulins' isotypes are present in breast milk, IgM and IgA are made locally in

(See figure on next page.)

Fig. 4 Neonates exposed to HIV have altered IgA-microbiota binding in stool. **A** Representative flow plot of bacteria flow cytometry in stool. Plots are from the same infant stool sample with a left panel showing IgA coating and the right showing IgM. **B** Percentage of IgA-bound bacteria in stool. **C** PCoA showing IgA-bound, IgA-unbound, and stool microbiota in nHEU and nHU infants. **D** Relative abundance of microbiota at phylum level comparing IgA-bound microbiota in stool and whole stool (input). **E** Alpha diversity of IgA bound microbiota in stool between nHEU and nHU. **F** Differentially abundant bacterial taxa in IgA bound fraction

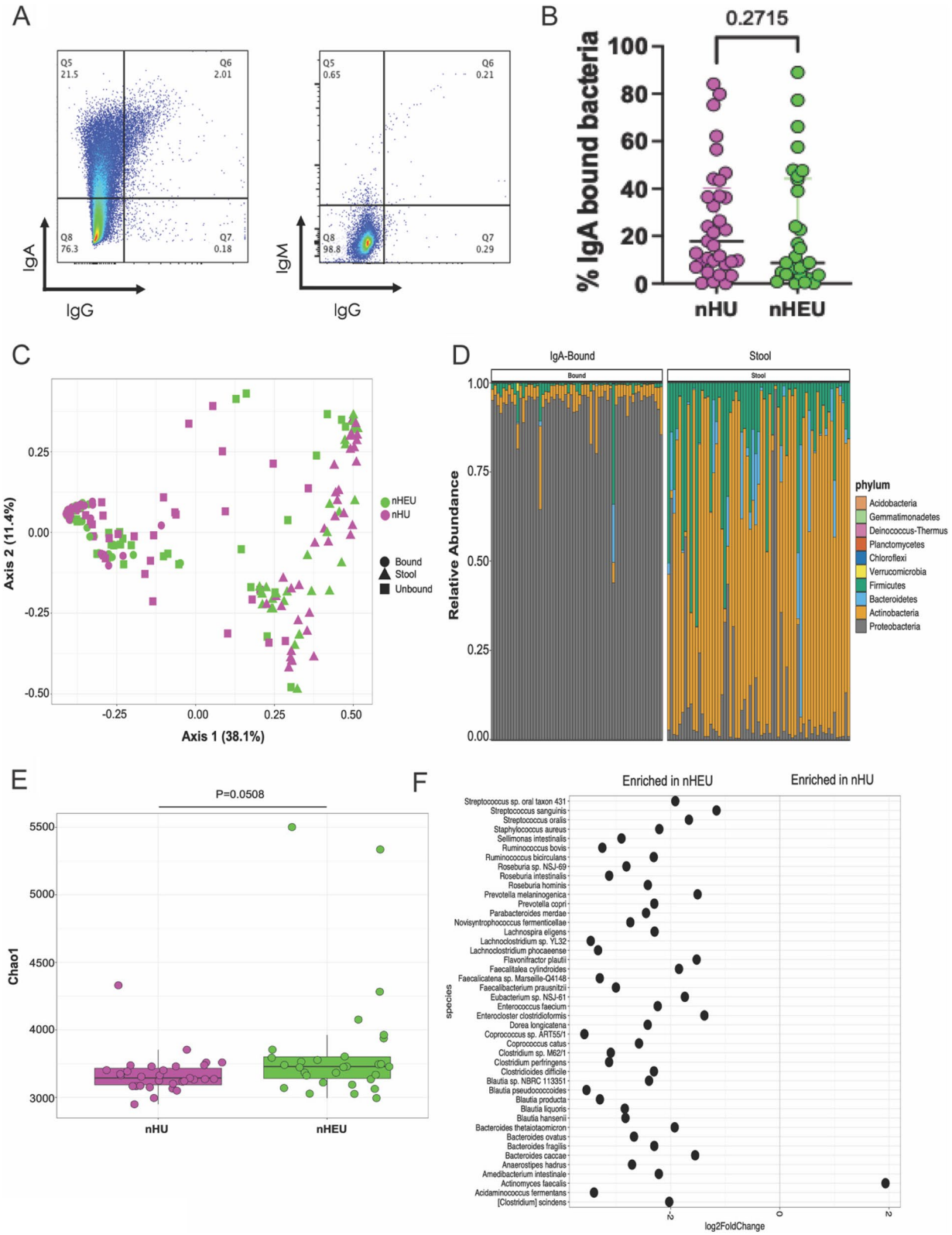

Fig. 4 (See legend on previous page.)

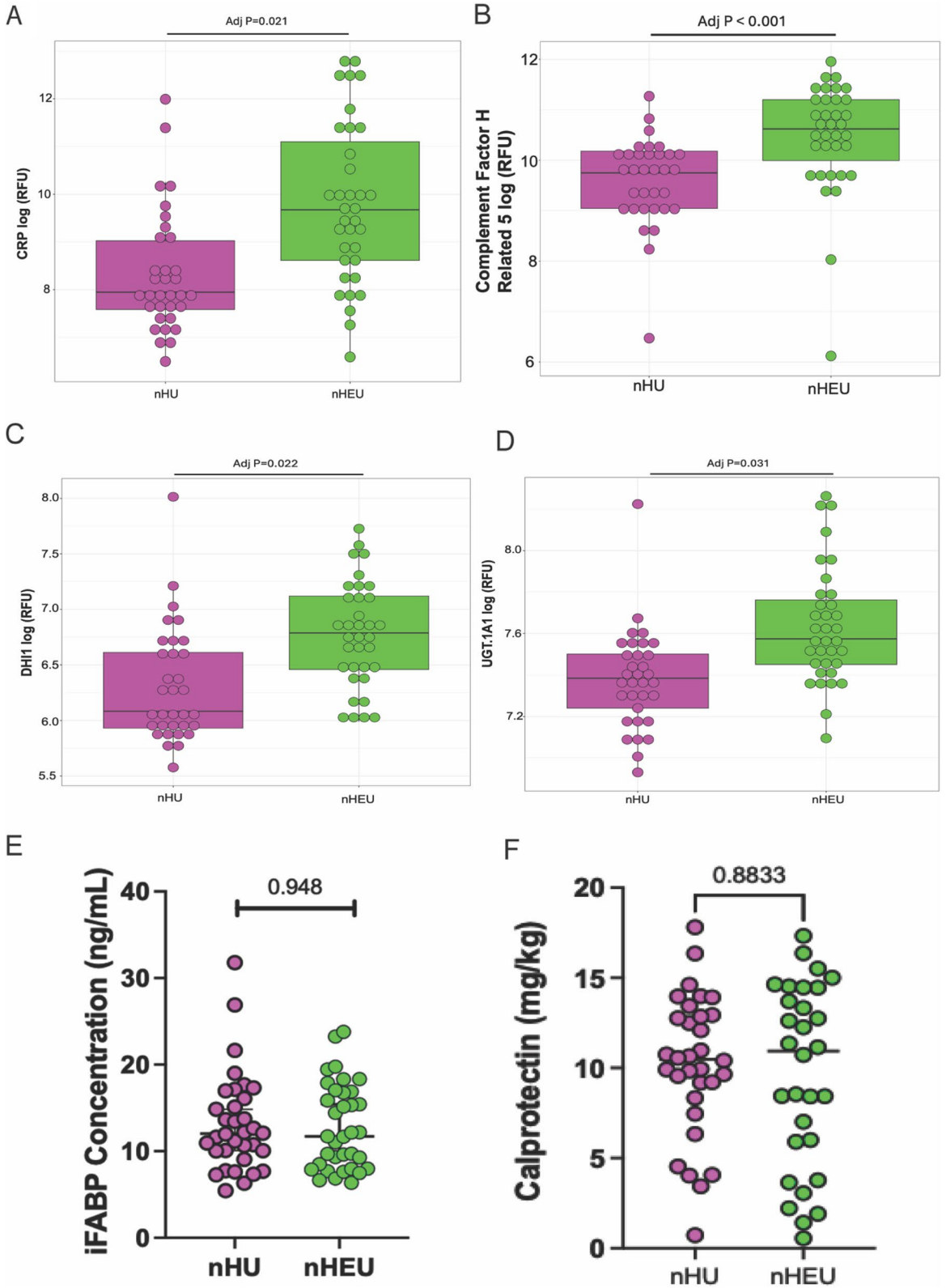

Fig. 5 Neonates exposed to HIV have heightened systemic inflammation at four weeks of age. **A**–**D** Concentrations of biomarkers in plasma measured by SomaScan assay. **E** iFABP concentration in infant plasma. The concentration of calprotectin in stool in nHEU and nHU. Comparisons with adjusted *p* values < 0.05 are significant

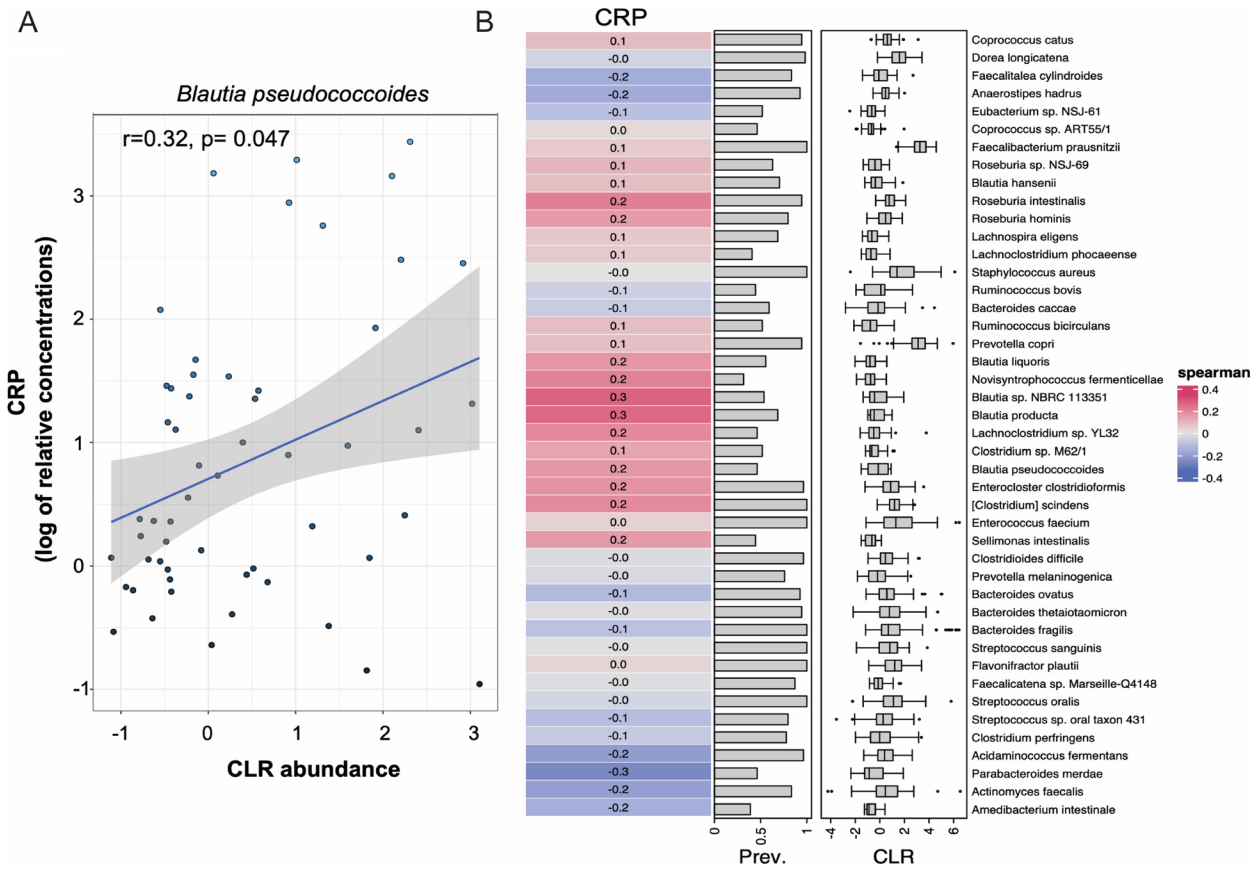

Fig. 6 Abundance of *Blautia* species positively correlated with plasma CRP. **A** Correlation between stool relative abundance of *Blautia pseudococcoides* and plasma CRP concentration. **B** Spearman correlation between the relative abundance of bacteria in IgA bound fraction and plasma CRP concentration

the mammary gland [63]. Therefore, it is not surprising that concentrations of these immunoglobulins in serum are not reflective of those in breast milk which is consistent with previous reports [64]. While we found no difference in the quantity of total immunoglobulins in breast milk, we did not assess the quality. Previous studies have demonstrated altered biophysical features of immunoglobulins in the serum of PLWH [65]. It is plausible that those traits may extend to breast milk-derived antibodies. We observed lower concentrations of total antibody in infant stool compared to breast milk consistent with prior reports [66], likely due to gastric digestion. However, we noted no difference in intestinal total antibody concentrations passively acquired by nHEU suggesting that there is no impact of HIV exposure on breast milk antibody transfer, although we did not measure immunoglobulin subclasses in neonatal stool.

nHEU had multiple bacterial taxa that were significantly differentially abundant compared to nHU. Findings on the bacterial microbiota of HIV-exposed infants have been highly variable across studies. For example, Bender et al. observed significantly lower alpha diversity in Haitian infants exposed to HIV compared to infants who were HIV unexposed at 4–10 weeks of age [9]. They also noted an enrichment of Pseudomonadaceae and Thermaceae in HIV-exposed infants. Similarly, in a study by Grant-Beurmann and colleagues, authors reported significantly lower alpha diversity in breastfeeding HIV-exposed infants compared to unexposed peers after aggregating data across multiple time points. They also observed a significantly lower abundance of *Bifidobacterium* at 6 months in HIV-exposed infants [7]. Here, we find an enrichment of various taxa including *Shigella, Staphylococcus, Klebsiella, Blautia,* and *Anaerostipes* species in exposed infants which have not been reported in previous studies. There are multiple reasons that explain the differences in the microbiome that we observed including the age of microbiota assessment, mode of delivery, and feeding. Moreover, these studies were conducted across different geographical locations which has been shown to impact the microbiota [67]. Most importantly, our study used shotgun DNA sequencing to assess

the bacteriome while the above studies used 16S rRNA amplicon sequencing. Shotgun sequencing has been shown to yield higher microbial resolution and accuracy compared to 16S rRNA amplicon sequencing [68]. We observed an enrichment of pathobionts in the gut of nHEU including *Klebsiella pneumoniae, Shigella flexneri, Hafnia alvei,* and *Staphylococcus aureus*. In contrast, nHU guts were enriched with *Bifidobacterium breve* and *Bacteroides thetaiotaomicron*which have been shown to provide multiple benefits to the pediatric host [69, 70].

Beyond the bacteriome, we also assessed the enteric DNA virome. To our knowledge, this is the first report that examines the virome in nHEU. *Pedovirus* and *Biseptimavirus* phages were enriched in nHEU versus nHU with their corresponding predicted bacterial hosts also elevated in nHEU. An increase in abundance of both the phage and its host suggests that the phage may not be lytic. Less killing by phage may allow for pathobionts such as *Escherichia coli* and others to persist in the gut. Our future studies will assess the kinetics of the association between the bacteriome and the virome in infants exposed to HIV. Nonetheless, we show for the first time that HIV exposure minimally impacts the enteric virome in the first month of life despite maternal and infant antiretroviral treatment. Whether the RNA virome may be more altered by HIV exposure is unknown.

We observed elevated concentrations of CRP in nHEU [49]. Dirajlal-Fargo et al. observed higher inflammatory markers including CRP in nHEU at birth although this was not evident at 6 months [6]. Similarly, Prendergast et al. reported elevated CRP at week 6 of life in HIV exposed versus unexposed Zimbabwean infants [57]. We also measured markers of intestinal inflammation and epithelial integrity. Concentrations of fecal calprotectin, which is a marker of intestinal inflammation and disease [71], were not significantly different between nHU and nHEU. Similarly, we found no difference in plasma concentrations of intestinal fatty acid binding protein (iFABP) between nHEU and nHU. In our previous analysis of the plasma of neonates from this cohort, we found iFABP, to be elevated in nHEU at birth but not at 36 weeks of age [72]. Our present findings are consistent with those of Prendergast et al. who found no difference in concentration of iFABP at 6 weeks of age between exposed and unexposed infants [57]. While it is plausible that intestinal inflammation may resolve within the first month based on the iFABP findings, it is important to note that these two markers alone may not provide a complete picture of intestinal inflammation. Calprotectin is released predominantly by neutrophils and may not fully capture inflammatory responses by other immune cells such as lymphocytes. Therefore, while our results suggest the absence of overt intestinal inflammation, we cannot conclusively rule out subtle inflammatory processes that might be detected using a broader panel of biomarkers or alternative methodologies.

The relative abundance of *B. pseudococcoides* was positively associated with concentrations of plasma CRP. This is consistent with previous work that has found associations between higher abundance of *Blautia spp* and inflammation [73, 74]. Other studies have observed a beneficial effect of various *Blautia* species on the host [75]. Most of these, however, have been conducted using adult humans or mice. It is unclear whether the reported effects of bacteria from this genus would have a similar impact on the pediatric host. Moreover, characterization has mostly been done at the genus level, and the effects of specific species or strains are less described. IgA-bound *Blautia* spp was also positively associated with CRP concentration. It is plausible that *Blautia spp* induces inflammation in nHEU although causality remains to be tested. Nonetheless, we find *B. pseudococcoides* in nHEU stool and IgA-bound *B. producta* to be associated with systemic inflammation.

We tested whether passively transferred IgA in nHEU affected bacterial growth differentially between nHEU versus nHU. While IgA from both MLWH and MLWoH could inhibit bacteria growth, that from MLWH displayed a significantly lower bacteriostatic effect compared to that from MLWoH. This is consistent with the finding that despite *B. pseudococcoides* being coated by IgA in nHEU, this bacterium was also enriched in their stool. These data show that IgA from MLWH has an impaired ability to inhibit the growth of specific (potentially inflammatory) gut bacteria which may explain heightened inflammation in nHEU. We observed no

(See figure on next page.)

Fig. 7 IgA in the breast milk of mothers living with HIV exhibits an impaired ability to inhibit the growth of specific gut commensals. *B. thetaiotaomicron* or *B. coccoides* were cultured in the presence of IgA purified from the breast milk of MLWoH or MLWH. Breast milk IgA from 5 mothers per group was used, and each participant's antibody was tested separately in triplicates. A total of six wells per bacteria were used as positive controls (no IgA). **A** Growth curve of *B. thetaiotaomicron* co-cultured with IgA purified from the breast milk of MLWH or MLWoH. **B** Growth curve of *B. coccoides* co-cultured with IgA purified from breast milk of MLWH or MLWoH. **C**, **D** Area under the curve for bacterial growth curves. **E**–**F** Levels of *B. thetaiotaomicron* and *B. coccoides* specific IgA in the breast milk of MLWH or MLWoH respectively. Data is shown as mean ± SEM

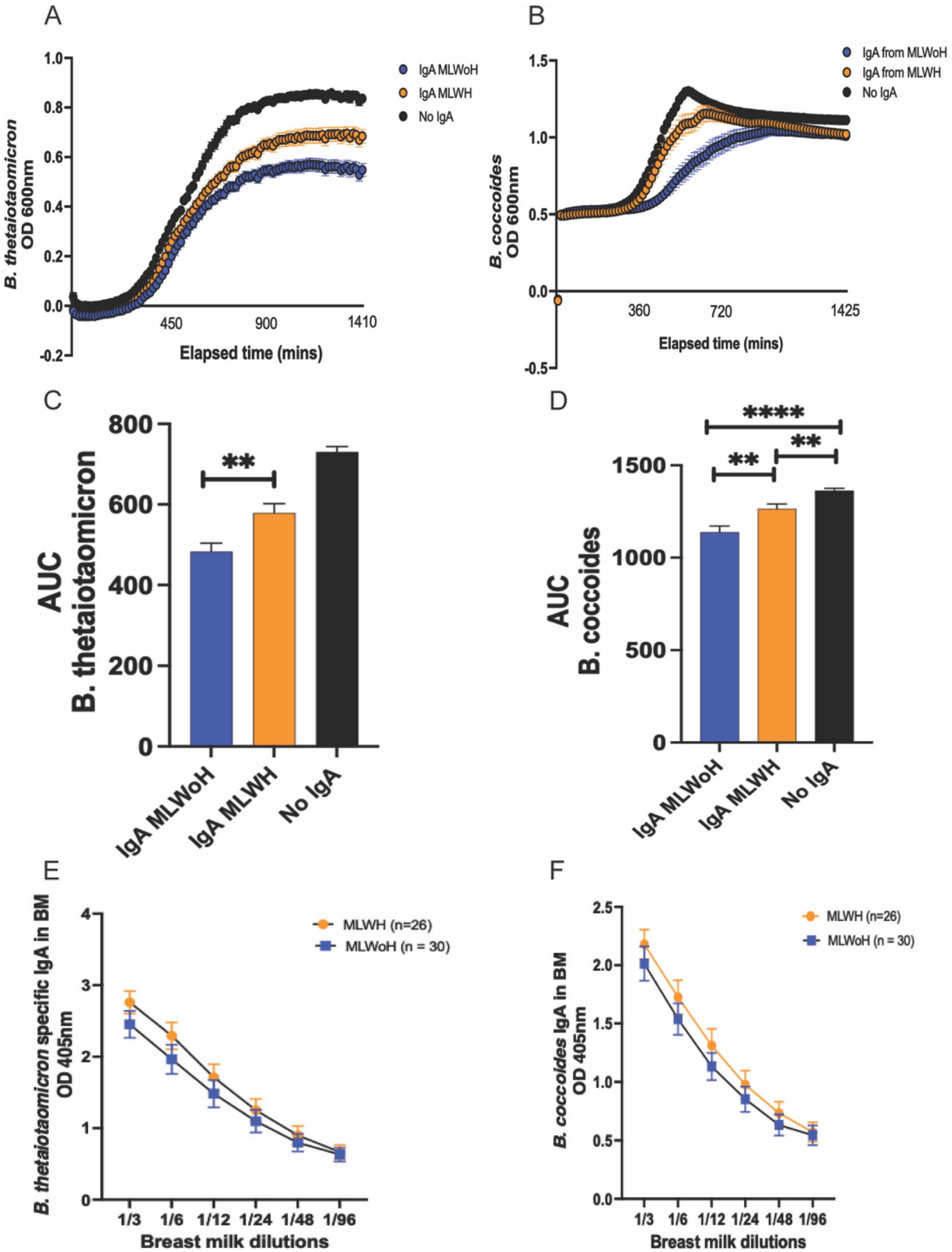

Fig. 7 (See legend on previous page.)

significant difference in the levels of microbiota-specific IgA in breast milk of MLWH compared to that from MLWoH. Therefore, despite having comparable titers of microbiota-specific IgA, this antibody has altered bacteriostatic function consistent with reports of abnormal B cell compartments in PLWH [76, 77].

While our study highlights significant differences in the gut bacteriome, virome, IgA-microbiota binding, and inflammation, some limitations are notable. nHEU are exposed to multiple factors including maternal antiretroviral therapy, HIV, and infant antiretroviral prophylaxis and it is difficult to assess how each of these exposures may contribute to the observed outcomes. However, in the modern era of universal antiretroviral therapy, our findings remain relevant to the typical clinical setting for nHEUs. Moreover, while we observed impaired breast milk IgA function in MLWH, there was no significant difference in total and commensal-specific IgA levels in the breast milk of MLWH compared to MLWoH. This suggests that qualitative differences in the antibody, such as glycosylation or specific function, rather than quantity, may underlie the observed outcome in infants. We did not extensively assess these maternal antibody features which could have provided further insights on the mechanisms behind altered bacteriostatic effect in IgA from MLWH.

Altogether, we find that mothers living with HIV have a comparable distribution of antibodies in breast milk to mothers living without HIV. Moreover, neonates exposed to HIV display profound alterations in their gut bacteriome; and gut abundance of *Blautia* species is associated with systemic inflammatory biomarkers. Moreover, we show that anti-commensal IgA in the breast milk of MLWH exhibits a significantly lower ability to limit the growth of potentially inflammatory bacteria which could be a mechanism behind altered gut microbiota and inflammation in nHEU.

Supplementary Information

The online version contains supplementary material available at https://doi.org/10.1186/s40168-024-01973-z.

Supplementary Material 1: Figure S1. Spearman correlation between centered-log ratio (CLR) transformed abundance of differentially abundant stool bacteria between nHEU and nHU and proteins elevated in the plasma of nHEU.

Supplementary Material 2: Table S1. Maternal and infant characteristics.

Supplementary Material 3: Table S2. Metabolic pathways in nHU and nHEU.

Supplementary Material 4: Table S3. Predicted hosts for differentially enriched enteric phages.

Acknowledgements
We would like to acknowledge the Research Scientific Computing core at Seattle Children's that provided access to the computing resources that contributed to the results reported here.

Authors' contributions
AB -performed experiments, data analysis and wrote manuscript C.D -data analysis and wrote manuscript B.B -data analysis and wrote manuscript S.G -data analysis and wrote manuscript B.A -wrote manuscript M.K -data analysis and wrote manuscript C.G -data analysis and wrote manuscript B.M -data analysis and wrote manuscript C.F -performed experiments H.J -data analysis and wrote manuscript. D.N -performed experiments, data analysis and wrote manuscript.

Funding
D.D.N thanks CFAR at the University of Washington for the New Investigator award (AI027757) and NICHD for the R21 award (R21HD106574).

Data availability
The stool metagenomic sequencing raw reads generated during this study are available at SRA under the accession number PRJNA1143669. The raw somalogic protein data and associated metadata files are available in Github (https://github.com/Nyangahu/Neonates_HIV_exposed).

Declarations

Ethics approval and consent to participate
Infants were recruited as part of an ongoing observational study of mother-infant pairs in Cape Town, South Africa [22]. The study was approved by the University of Cape Town's Human Research Ethics Committee (reference 285/2012).

Consent for publication
This declaration is not applicable.

Competing interests
The authors declare that they have no competing interests.

Received: 31 July 2024 Accepted: 11 November 2024
Published online: 20 December 2024

References

1. UNAIDS. Fact Sheet-World AIDS Day 2017. Geneva: UN Joint Programme on HIV/AIDS (UNAIDS); Programme on HIV/AIDS. 2017. 978–92–9173–945–5.
2. Weinberg A, et al. Factors associated with lower respiratory tract infections in HIV-exposed uninfected infants. AIDS Res Hum Retroviruses. 2018;34:527–35.
3. Slogrove AL, Cotton MF, Esser MM. Severe infections in HIV-exposed uninfected infants: clinical evidence of immunodeficiency. J Trop Pediatr. 2010;56:75–81.
4. Abu-Raya B, Kollmann TR, Marchant A, MacGillivray DM. The immune system of HIV-exposed uninfected infants. Front Immunol. 2016;7:1–10.
5. Lohman-Payne B, et al. HIV-exposed uninfected infants: elevated cord blood Interleukin 8 (IL-8) is significantly associated with maternal HIV infection and systemic IL-8 in a Kenyan cohort. Clin Transl Med. 2018;7:26.
6. DirajIal-Fargo S, et al. HIV-exposed-uninfected infants have increased inflammation and monocyte activation. AIDS. 2019;33:845–53.
7. Grant-Beurmann S, et al. Dynamics of the infant gut microbiota in the first 18 months of life: the impact of maternal HIV infection and breastfeeding. Microbiome. 2022;10.
8. Machiavelli A, Duarte RTD, Pires MM de S, Zárate-Bladés CR, Pinto AR. The impact of in utero HIV exposure on gut microbiota, inflammation, and microbial translocation. Gut Microbes. 2019;10:599–614.
9. Bender JM, et al. Maternal HIV infection influences the microbiome of HIV-uninfected infants. Sci Transl Med. 2016;8:349ra100.

10. Durazzi F, et al. Comparison between 16S rRNA and shotgun sequencing data for the taxonomic characterization of the gut microbiota. Sci Rep. 2021;11.
11. Cao Z, et al. The gut virome: a new microbiome component in health and disease-NC-ND license. 2022.
12. Nyangahu DD, et al. I M M U N O LO G Y Bifidobacterium Infantis Associates with T Cell Immunity in Human Infants and Is Sufficient to Enhance Antigen-Specific T Cells in Mice. 2023. https://www.science.org.
13. Lessen R, Kavanagh K. Position of the academy of nutrition and dietetics: promoting and supporting breastfeeding. J Acad Nutr Diet. 2015;115:444–9.
14. Tha-In T, Bayry J, Metselaar HJ, Kaveri SV, Kwekkeboom J. Modulation of the cellular immune system by intravenous immunoglobulin. Trends in Immunology Preprint at. 2008. https://doi.org/10.1016/j.it.2008.08.004.
15. McGowan JP, et al. Relationship of serum immunoglobulin and IgG subclass levels to race, ethnicity and behavioral characteristics in HIV infection. 2006.
16. Lugada ES, et al. Immunoglobulin levels amongst persons with and without human immunodeficiency virus type 1 infection in Uganda and Norway. Scand J Immunol. 2004;59:203–8.
17. Baroncelli S, et al. IgG abnormalities in HIV-positive Malawian women initiating antiretroviral therapy during pregnancy persist after 24 months of treatment. Int J Infect Dis. 2019;88:1–7.
18. Koch MA, et al. Maternal IgG and IgA antibodies dampen mucosal T helper cell responses in early life. Cell. 2016;165:827–41.
19. Palm NW, et al. Immunoglobulin A coating identifies colitogenic bacteria in inflammatory bowel disease. PMC. 2014;158:1000–10.
20. Fadlallah J, et al. Synergistic convergence of microbiota-specific systemic IgG and secretory IgA. Journal of Allergy and Clinical Immunology. 2019;143:1575–1585.e4.
21. Kiravu A, et al. Bacille calmette-guérin vaccine strain modulates the ontogeny of both mycobacterial-specific and heterologous T cell immunity to vaccination in infants. Front Immunol. 2019;10:1–11.
22. Kidzeru EB, et al. In-utero exposure to maternal HIV infection alters T-cell immune responses to vaccination in HIV-uninfected infants. 2014;19:161–9.
23. National Department of Health. National Consolidated Guidelines for the Prevention of Mother-To-Child Transmission of HIV (PMTCT) and the Management of HIV in Children, Adolescents and Adults. Dep Health Republic South Afr. 2015;1–128.
24. Wilmore JR, et al. Commensal microbes induce serum IgA responses that protect against polymicrobial sepsis. Cell Host Microbe. 2018;23:302–311.e3.
25. Chen S, Zhou Y, Chen Y, Gu J. Fastp: an ultra-fast all-in-one FASTQ preprocessor. Bioinformatics. 2018;34:i884–90.
26. Wood DE, Salzberg SL. Kraken: Ultrafast metagenomic sequence classification using exact alignments. 2014.
27. Lu J, Breitwieser FP, Thielen P, Salzberg SL. Bracken: estimating species abundance in metagenomics data. PeerJ Comput Sci. 2017;2017.
28. McMurdie PJ, Holmes S. Phyloseq: an R package for reproducible interactive analysis and graphics of microbiome census data. PLoS ONE. 2013;8:e61217.
29. Martin BD, Witten D, Willis AD. Modeling microbial abundances and dysbiosis with beta-binomial regression. https://doi.org/10.1214/19-AOAS1283SUPPA.
30. Love MI, Huber W, Anders S. Moderated estimation of fold change and dispersion for RNA-seq data with DESeq2. Genome Biol. 2014;15:1–21.
31. Beghini F, et al. Integrating taxonomic, functional, and strain-level profiling of diverse microbial communities with bioBakery 3. Elife. 2021;10.
32. Prjibelski A, Antipov D, Meleshko D, Lapidus A, Korobeynikov A. Using SPAdes De Novo Assembler. Curr Protoc Bioinformatics. 2020;70.
33. Camargo AP, et al. Identification of mobile genetic elements with geNomad. Nat Biotechnol. 2023. https://doi.org/10.1038/s41587-023-01953-y.
34. Hauser M, Steinegger M, Söding J. MMseqs software suite for fast and deep clustering and searching of large protein sequence sets. Bioinformatics. 2016;32:1323–30.
35. Kieft K, Zhou Z, Anantharaman K. VIBRANT: automated recovery, annotation and curation of microbial viruses, and evaluation of viral community function from genomic sequences. Microbiome. 2020;8.
36. Kim CH. et al. Stability and reproducibility of proteomic profiles measured with an aptamer-based platform. Sci Rep. 2018;8.
37. Ritchie ME, et al. Limma powers differential expression analyses for RNA-sequencing and microarray studies. Nucleic Acids Res. 2015;43:e47.
38. Michaud E, et al. Alteration of microbiota antibody-mediated immune selection contributes to dysbiosis in inflammatory bowel diseases. EMBO Mol Med. 2022;14.
39. Claassen-Weitz S, et al. HIV-exposure, early life feeding practices and delivery mode impacts on faecal bacterial profiles in a South African birth cohort. Sci Rep. 2018;8.
40. Provisional WHO/UNAIDS Recommendations on the Use of Cotrimoxazole Prophylaxis in Adults and Children Living with HIV/ AIDS in Africa. 2001.
41. Breiman L. Random forests. Mach Learn. 2001;45:5–32.
42. Mallick H, et al. Multivariable association discovery in population-scale meta-omics studies. PLoS Comput Biol. 2021;17.
43. Leal Rodríguez C, et al. The infant gut virome is associated with preschool asthma risk independently of bacteria. Nat Med. 2024;30:138–48.
44. Roux, S. et al. iPHoP: an integrated machine learning framework to maximize host prediction for metagenome-derived viruses of archaea and bacteria. PLoS Biol. 2023;21.
45. Bushman F, Liang G. Assembly of the virome in newborn human infants. Curr Opinion Virol. 2021;48:17–22. Preprint at https://doi.org/10.1016/j.coviro.2021.03.004.
46. Weis AM, Round JL. Microbiota-antibody interactions that regulate gut homeostasis. Cell Host Microbe. 2021;29:334–46.
47. Dinh DM, et al. Intestinal Microbiota, microbial translocation, and systemic inflammation in chronic HIV infection. J Infect Dis. 2015;211:19–27 Oxford University Press, 2015.
48. Lobionda S, Sittipo P, Kwon HY, Lee YK. The role of gut microbiota in intestinal inflammation with respect to diet and extrinsic stressors. Microorganisms. 2019;7. Preprint at https://doi.org/10.3390/microorganisms7080271.
49. Sproston NR, Ashworth JJ. Role of C-reactive protein at sites of inflammation and infection. Front Immunol. 2018;9. Preprint at https://doi.org/10.3389/fimmu.2018.00754.
50. Iglesias MJ, et al. Elevated plasma complement factor H related 5 protein is associated with venous thromboembolism. Nat Commun. 2023;14.
51. Medjeral-Thomas NR, et al. Glomerular complement factor H–related protein 5 (FHR5) is highly prevalent in C3 glomerulopathy and associated with renal impairment. Kidney Int Rep. 2019;4:1387–400.
52. Odermatt A, Arnold P, Stauffer A, Frey BM, Frey FJ. The N-terminal anchor sequences of 11-hydroxysteroid dehydrogenases determine their orientation in the endoplasmic reticulum membrane*. 1999.
53. Jon FW. Neonatal Indirect Hyperbilirubinemia and Kernicterus. 2018;1198–218.
54. Wells JM, et al. Homeostasis of the gut barrier and potential biomarkers. Am J Physiol Gastrointestinal Liver Physiol. 2017;312:G171–93. Preprint at https://doi.org/10.1152/ajpgi.00048.2015.
55. Sikora M, et al. Intestinal fatty acid binding protein, a biomarker of intestinal barrier, is associated with severity of psoriasis. J Clin Med. 2019;8.
56. Wiercinska-Drapalo A, Jaroszewicz J, Siwak E, Pogorzelska J, Prokopowicz D. Intestinal fatty acid binding protein (I-FABP) as a possible biomarker of ileitis in patients with ulcerative colitis. Regul Pept. 2008;147:25–8.
57. Prendergast AJ, et al. Intestinal damage and inflammatory biomarkers in human immunodeficiency virus (HIV)-exposed and HIV-infected Zimbabwean infants. J Infect Dis. 2017;216:651–61.
58. Bunker JJ, et al. Natural polyreactive IgA antibodies coat the intestinal microbiota. Science (1979). 2017;358.
59. Boudry G, et al. The relationship between breast milk components and the infant gut microbiota. Front Nutr. 2021;8. Preprint at https://doi.org/10.3389/fnut.2021.629740.
60. Guo J, et al. Role of IgA in the early-life establishment of the gut microbiota and immunity: Implications for constructing a healthy start. Gut Microbes. 2021;13:1–21. Preprint at https://doi.org/10.1080/19490976.2021.1908101.
61. Maturana JL, Cárdenas JP. Insights on the evolutionary genomics of the Blautia genus: potential new species and genetic content among lineages. Front Microbiol. 2021;12.

62. Raux M, et al. IgG subclass distribution in serum and various mucosal fluids of HIV type 1-infected subjects. AIDS Res Hum Retroviruses. 2000;16:583–94.
63. Hassiotou F, Geddes DT, Hartmann PE. Cells in human milk: State of the science. J Hum Lact. 2013;29:171–82.
64. Pullen KM, et al. Selective functional antibody transfer into the breastmilk after SARS-CoV-2 infection. Cell Rep. 2021;37.
65. Taylor SA, et al. HIV-associated alterations of the biophysical features of maternal antibodies correlate with their reduced transfer across the placenta. J Infect Dis. 2022;226:1441–50.
66. Demers-Mathieu V, Underwood MA, Beverly RL, Nielsen SD, Dallas DC. Comparison of human milk immunoglobulin survival during gastric digestion between preterm and term infants. Nutrients. 2018;10.
67. Iwase SC, et al. Longitudinal gut microbiota composition of South African and Nigerian infants in relation to tetanus vaccine responses. Microbiol Spectr. 2024;12.
68. Brumfield KD, Huq A, Colwell RR, Olds JL, Leddy MB. Microbial resolution of whole genome shotgun and 16S amplicon metagenomic sequencing using publicly available NEON data. PLoS One. 2020;15.
69. Varyukhina S, et al. Glycan-modifying bacteria-derived soluble factors from Bacteroides thetaiotaomicron and Lactobacillus casei inhibit rotavirus infection in human intestinal cells. Microbes Infect. 2012;14:273–8.
70. Bozzi Cionci NC, Baffoni L, Gaggìa F, Di Gioia D. Therapeutic microbiology: The role of bifidobacterium breve as food supplement for the prevention/treatment of paediatric diseases. Nutrients. 2018;10. Preprint at https://doi.org/10.3390/nu10111723.
71. Bunn SK, Bisset WM, Main MJC, Golden BE. Fecal calprotectin as a measure of disease activity in childhood inflammatory bowel disease. J Pediatr Gastroenterol Nutr. 2001;32:171–7.
72. Dzanibe S, Jaspan HB, Zulu MZ, Kiravu A, Gray CM. Impact of maternal HIV exposure, feeding status, and microbiome on infant cellular immunity. J Leukoc Biol. 2019;105:281–9.
73. Nishino K, et al. Analysis of endoscopic brush samples identified mucosa-associated dysbiosis in inflammatory bowel disease. J Gastroenterol. 2018;53:95–106.
74. Kumbhari A, et al. Discovery of disease-adapted bacterial lineages in inflammatory bowel diseases. Cell Host Microbe. 2024;32:1147–1162.e12.
75. Liu X, et al. Blautia—a new functional genus with potential probiotic properties? Gut Microbes. 2021;13:1–21. Preprint at https://doi.org/10.1080/19490976.2021.1875796.
76. Titanji K, et al. Primary HIV-1 infection sets the stage for important B lymphocyte dysfunctions.
77. Moir S, Fauci AS. B cells in HIV infection and disease Susan. Nat Rev Immunol. 2009;9:235–45.

Publisher's Note